Soft Matter

RSC Publishing

COMMUNICATION

View Article Online
View Journal

Fluid–solid transitions in soft-repulsive colloids†

Cite this: DOI: 10.1039/c2sm27654b

Divya Paloli,[ab] Priti S. Mohanty,*[a] Jérôme J. Crassous,[ab] Emanuela Zaccarelli[c] and Peter Schurtenberger[a]

Received 17th November 2012
Accepted 19th December 2012

DOI: 10.1039/c2sm27654b

www.rsc.org/softmatter

We use monodisperse poly(*N*-isopropylacrylamide) (PNIPAM) microgels as a model system for soft repulsive colloids and study their density dependent structural ordering and phase behaviour using confocal laser scanning microscopy (CLSM). The experiments are carried out at low temperatures, where the particles are in the swollen state and interact *via* a Hertzian potential, evidenced through a quantitative comparison of the pair correlation functions $g(r)$ obtained with CLSM and computer simulations. We worked over a broad range of effective volume fractions ϕ_{eff} below and above close packing (ϕ_{cp}). CLSM allows us to identify a fluid–glass and a fluid–crystal transition by looking at the structure and dynamics of the suspensions. The density dependent $g(r)$ values exhibit clearly visible anomalies at high $\phi_{\text{eff}} > \phi_{\text{cp}}$ which we interpret as a structural signature of the glass transition related to the particle softness. These results are discussed in light of the previously studied phase behaviour of colloidal systems interacting with hard and soft repulsive interaction potentials.

Hard sphere colloids have frequently been used as model systems in condensed matter physics to address density driven fluid–crystal and fluid–glass transitions.[1–6] Recently, the focus of the theoretical and experimental soft matter community has increasingly shifted to soft repulsive colloids,[7–17] where the interaction potential shows a finite repulsion at or beyond contact ($a_s \leq \sigma$, with a_s the center-to-center distance and σ the particle diameter). As a result of particle softness, interesting equilibrium and non-equilibrium phases have been observed in theoretical studies of soft-repulsive colloids. The most important findings include a non-monotonic density dependence of the freezing transition[10–12,18] with a complex array of crystalline structures,[15,16] a shift of the glass line to higher effective volume fractions ϕ_{eff} with increasing softness,[13,14] and a density driven re-entrant fluid–glass–fluid transition.[17] However, the complexity of this theoretically predicted phase behaviour has not yet been reproduced by the corresponding experimental studies.

In the experimental effort devoted to soft repulsive colloids, cross-linked poly(*N*-isopropylacrylamide) (PNIPAM)-based microgels have been frequently used as an ideal model system, where the particle softness can not only be tuned through the crosslink density during the synthesis, but also in a completely reversible fashion through the response of the polymer to variations in temperature, pH, ionic strength or hydrostatic pressure.[19–21] Neutral,[22–28] charged[29–35] and core–shell PNIPAM-based microgels[36,37] have previously been used, and their concentration and temperature dependent properties and phase behaviour have been extensively investigated. These studies have clearly shown the existence of much richer phase behaviour when compared to simple hard sphere colloids. Particularly noteworthy has been the observation that due to the softness of the particles, microgels can be packed to effective volume fractions far above close packing, ϕ_{cp}, with enormous consequences for the resulting structural and dynamical properties.[22–26] However, a major problem until now has clearly been the lack of knowledge on the exact nature of the interaction potential between the various types of microgels, and on its ϕ_{eff} dependence at high packing fractions.

A number of experimental studies on PNIPAM microgel dispersions have already been reported on attempts to determine the nature of the interaction potential. The inverse power law (*i.e.* $U(r) \propto r^{-n}$) and brush-like interactions were found to be in excellent agreement with the ϕ_{eff} dependence of the shear modulus (G_p) in concentrated microgel suspensions based on rheological studies[27] and diffusing wave spectroscopy[23] respectively. Recently a number of studies have been proposed to model soft-colloids using a pair-wise additive Hertzian potential[16,17,22] which was initially derived for the description of the elastic repulsion between deformable soft colloids. This was for example used to understand the structural signature of the

---

[a] *Physical Chemistry, Department of Chemistry, Lund University, Lund, Sweden. E-mail: priti.mohanty@fkem1.lu.se*

[b] *Department of Chemistry, University of Fribourg, Fribourg, Switzerland*

[c] *CNR-ISC and Dipartimento di Fisica, Università di Roma La Sapienza, Rome, Italy*

† Electronic supplementary information (ESI) available. See DOI: 10.1039/c2sm27654b

jamming transition at finite temperatures, and its relationship to dynamical arrest and glass transition in PNIPAM microgels through experiments[22] on two-dimensional binary suspensions of microgels at high densities ($>\phi_{\rm cp}$). The observed structural features were found to be in agreement with simulations using Hertzian spheres. However, there is still a clear lack of conclusive experimental tests of the existing theoretical predictions for the properties of soft particle suspensions at and above close packing as a function of the softness of the potential.

Here we report experimental results for PNIPAM microgels, where we focus on the existence of possible equilibrium and non-equilibrium fluid–solid transitions and characterize the interparticle interaction potential of these systems. In particular, we investigate the presence of a glass transition and characterize the structure of the suspensions as given by the pair correlation function $g(r)$ both in the fluid as well as in the glassy states over an extended range of volume fractions. We show that $g(r)$ exhibits two distinct structural signatures of the glass transition related to the softness of the particles, and discuss our findings in view of the existing theoretical predictions for soft particles.

We used almost monodisperse PNIPAM microgels (polydispersity = 4%) with 5 mol% cross-linking density as a model system for soft colloids. Cross-linked PNIPAM microgels were synthesized using free-radical precipitation polymerization. Methacryloxyethyl thiocarbamoylrhodamine B (MRB) was used to covalently label the microgel particle. Details of the synthesis and purification methods are described elsewhere[19] and summarized in the ESI.† The particles were characterized using dynamic light scattering, and a summary of their swelling behaviour as a function of temperature can be found in the ESI, Fig. S1.† Effective volume fractions were determined using $\phi_{\rm eff} = n_{\rm p}(4/3)\pi R_{\rm eff}^{\;3}$, where $R_{\rm eff} = 357$ nm and $n_{\rm p}$ is the number density directly obtained by CLSM. In the current study, we worked at a constant temperature $T = 15$ °C and varied the number density to perform experiments over a broad range of effective volume fractions $0.1 \leq \phi_{\rm eff} \leq 1.5$. This distinguishes our study from other investigations, where the temperature responsiveness of the microgel size has been used as an elegant way to vary $\phi_{\rm eff}$.[22–24] Our approach however ensures that the particle softness is not altered as a result of temperature-induced de-swelling when $\phi_{\rm eff}$ is varied.

In order to ensure proper mixing and the absence of residual heterogeneities at high densities in the glassy state, samples were always homogenized at elevated temperatures where the corresponding particle de-swelling results in low values of $\phi_{\rm eff}$ and the suspensions have accordingly low viscosities. The samples were then quenched to the final temperature $T = 15$ °C. Fig. 1 summarizes our observations at all densities investigated. At low $\phi_{\rm eff}$, our suspensions are in a disordered fluid state, and the first two CLSM snapshots in Fig. 1 show the corresponding samples at effective volume fractions of $\phi_{\rm eff} = 0.26$ and $\phi_{\rm eff} = 0.52$, respectively. While samples for $\phi_{\rm eff} \leq 0.52$ remained in a fluid state, crystallization occurred for $\phi_{\rm eff} > 0.52$. This is also illustrated in Fig. 1, where the last three images in the upper row show examples of samples in the fluid–crystal coexistence region ($\phi_{\rm eff} = 0.56$) and the crystal region at $\phi_{\rm eff} = 0.61$ and $\phi_{\rm eff} = 0.9$, respectively. A detailed analysis of the crystalline samples suggests that the crystal structure, present for $\phi_{\rm eff} \geq 0.56$, is a mixture of fcc and hcp, similar to what has been reported for hard sphere colloids and also for neutral and charged microgels.[29,33–35,43,44] However, for the samples at the highest values of $\phi_{\rm eff}$ crystals only form when given sufficient time to nucleate and grow, or when using prolonged annealing at higher temperatures. In contrast, when performing fast quenches from the fluid state at higher temperatures the samples become arrested in a glassy amorphous phase as shown in the bottom row of Fig. 1 for $\phi_{\rm eff} = 0.77$, 0.97 and 1.44, respectively. The occurrence of a glass transition is also seen from the measurements of the particle mean square displacement $\langle \Delta r(t)^2 \rangle$ (see ESI, Fig. S3†), where we observe a transition between $\phi_{\rm eff} = 0.56$ and $\phi_{\rm eff} = 0.74$.

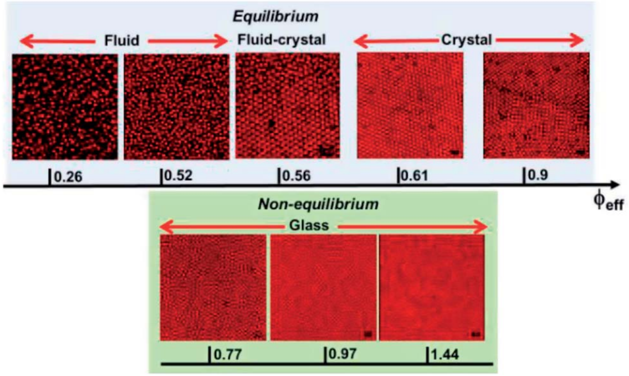

Fig. 1 Experimental phase diagram, together with CLSM snapshots at different $\phi_{\rm eff}$ at 15 °C taken in the fluid, crystalline and glassy states, respectively. Glassy states were obtained by fast quenches from the fluid state at higher temperature to 15 °C. The higher temperature is varied between 30 and 32 °C depending on the density in order to achieve the fluid state below freezing $\phi_{\rm eff}$.

We measured the density-dependent $g(r)$s for all values of $\phi_{\rm eff}$ investigated (Fig. 2). For $\phi_{\rm eff} = 0.56$ the equilibrium state of the sample is a fluid–crystal coexistence, and $g(r)$ is thus obtained by melting the crystalline state. At the lowest $\phi_{\rm eff} = 0.154$, $g(r)$ has a weak first peak and saturates to one at higher r-values, thus exhibiting the typical signature of a weakly correlated liquid state. With increasing $\phi_{\rm eff}$, $g(r)$ shows a systematic increase in the height of the first peak and also exhibits a broad second peak, indicating increasing spatial correlation among the particles. As shown in the ESI (Fig. S2†) and described in detail elsewhere,[38] the measured $g(r)$s are in quantitative agreement with computer (MD) simulations and liquid state integral equation calculations performed using the Rogers–Young closure relationship for particles interacting *via* a repulsive Hertzian potential given by $U(r) = \varepsilon(1 - r/\sigma)^{2.5}$ for $r \leq \sigma$, where ε is the strength of the potential and σ is the diameter of the particle. The Hertzian potential was found to remain independent at all densities in the fluid regime ($0.154 \leq \phi_{\rm eff} \leq 0.52$). Our results thus unambiguously demonstrate that the interaction between microgels is well described by a simple Hertzian potential (Fig. S2, ESI†) with a constant particle diameter $\sigma = 0.714$ µm, and strength $\varepsilon = 496k_{\rm B}T$ throughout the fluid regime.

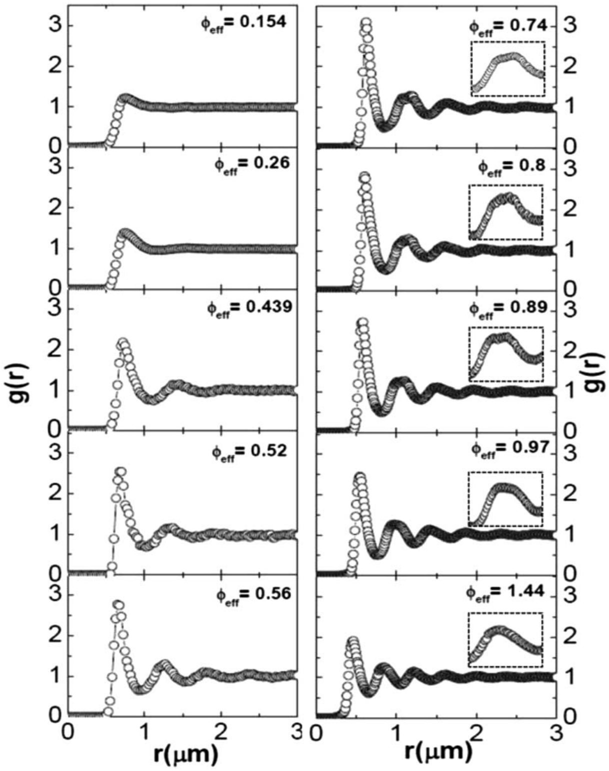

Fig. 2 Measured pair-correlation functions $g(r)$ at different ϕ_{eff} in the disordered fluid and glassy state below and above ϕ_{cp}. Inset: magnified view of the second peak of $g(r)$ showing a split or distortion, which is often used as a possible signature to identify colloidal glasses.

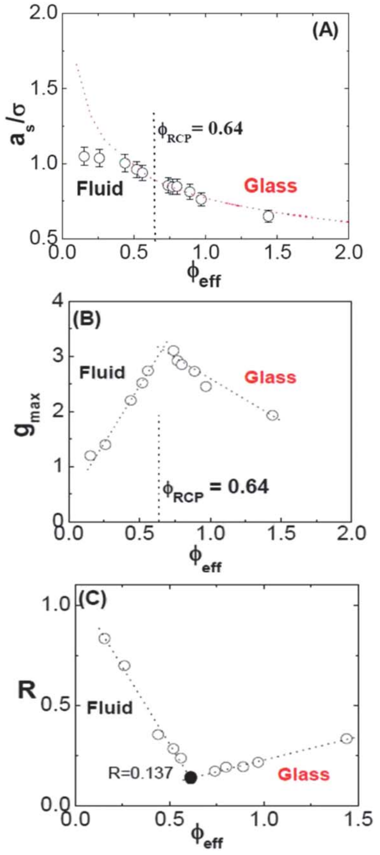

Fig. 3 (A) Average interparticle distance a_s calculated from the first peak position of $g(r)$ as a function of ϕ_{eff}. The red dotted line corresponds to the power law, $a_s/\sigma \propto (n_p)^{-1/3}$. (B) The height of the first peak of $g(r)$, g_{max}, as a function of ϕ_{eff}. (C) The ratio "$R = g_{\text{min}}/g_{\text{max}}$" *vs.* ϕ_{eff}, where g_{min} is the first minimum of $g(r)$.

Next, we analyse the structural ordering at high densities at and above the glass transition obtained by rapidly quenching the concentrated microgel suspension from elevated temperature (between 30 and 32 °C depending on the density) to 15 °C. Before all the measurements, the samples are equilibrated for 30–40 minutes. The density dependent $g(r)$s obtained at different ϕ_{eff} ($>\phi_{\text{cp}}$) (Fig. 2) have pronounced first and second order peaks and also exhibit weak higher order peaks.

It is interesting to compare these $g(r)$s with those obtained for hard sphere glasses.[3–5] Such a comparison is of course only possible in the vicinity of the glass transition, as hard spheres cannot compress or interpenetrate and states with $\phi_{\text{eff}} \gg \phi_{\text{cp}}$ are thus not possible. This becomes evident when looking at the average interparticle separation a_s (Fig. 3A) in units of the particle diameter σ where a_s is given by the position of the first peak of $g(r)$. While it initially remains almost constant at $a_s/\sigma \approx 1$ similar to what is observed for hard spheres, it significantly decreases at high $\phi_{\text{eff}} > \phi_{\text{cp}}$ to much lower values $a_s/\sigma < 1$, following a power law of the form $a_s/\sigma \propto (\phi_{\text{eff}})^{-1/3}$. For $\phi_{\text{eff}} > \phi_{\text{cp}}$, a_s is thus primarily determined by the number density n_p, which demonstrates the soft nature of the potential. When looking in detail at $g(r)$, it becomes immediately apparent that for the soft microgels the peak height is smaller and the peak width is broader than what is commonly found for hard spheres.

Colloidal hard sphere glasses exhibit a distorted flattened or split second peak for $g(r)$,[3,5] which can be directly linked to the dense random packing in the glass as demonstrated by Finney.[41] A split second peak is also found for charged[42] colloids or in atomic systems interacting with a Lennard-Jones potential,[40] and it has also been observed theoretically[39] and in simulations[17] for glasses formed by Hertzian spheres. It has been suggested to use this feature as a signature of a particle glass to identify colloidal glasses structurally. For our soft particles we indeed also find a similar behaviour for the glassy systems in the vicinity of the glass transition as demonstrated by the data shown in the insets in Fig. 2 for $\phi_{\text{eff}} \geq 0.74$. However, with increasing ϕ_{eff} this feature disappears and the second peak of $g(r)$ becomes again smooth. At the same time, the height of the first peak, g_{max}, passes through a maximum at the glass transition and then decreases (Fig. 3B). This non-monotonic behaviour can be explained by the fact that at higher volume fractions ($\phi_{\text{eff}} > \phi_{\text{cp}}$), it becomes increasingly difficult to find configurations with no overlap and to minimize the free energy. Hence to effectively create more space, the microgels can either shrink or interpenetrate and thus create a larger number of accessible configurations. This leads to a loss of positional correlation that is reflected in the broadening and decrease of the height of the peak.

A similar behaviour in $g(r)$ has already been reported for a 2D binary system of microgels, and was then related to the thermal vestige of the zero-temperature jamming transition.[22] However, when quantitatively comparing the 2D data with our own bulk 3D measurements, the high density 2D $g(r)$ appear to be much sharper, and have a much higher first peak height than our own 3D $g(r)$. Furthermore, the splits in the second peak are also quite pronounced for the 2D data. These differences could arise as a result of the 2D confinement or due to the temperature change that was adopted in ref. 22 in order to vary ϕ_{eff}.

We also look into the empirical criterion developed by Wendt and Abraham that links structural correlations to the location of the glass transition.[40] They suggested that the empirical parameter $R = g_{\min}/g_{\max}$, where $g_{\min}$ is the value of $g(r)$ at its first minimum, has a value of 0.14 at the glass transition. This criterion for example had been used previously to locate the glass transition in simulations of charged colloids.[42] The plot of R *vs.* ϕ_{eff} shown in Fig. 3C demonstrates the existence of two regimes with different slopes, separating the fluid and glassy states, and intersecting at a value of $R = 0.137$. When we use this point as another structural signature of the glass transition, we then obtain a corresponding value of $\phi_g \approx 0.65$. The maximum in $g_{\max}$ *vs.* ϕ_{eff}, and the minimum in R *vs.* ϕ_{eff} are thus both consistent with the existence of structural signatures of the glass transition for soft particles. The yield values of the glass transition ϕ_g are in good agreement with the location of ϕ_g from dynamic measurements of $\langle \Delta r(t)^2 \rangle$. The glass transition thus appears to be shifted slightly to higher values of ϕ_{eff} when compared to hard spheres, consistent with theoretical predictions of the glass transition with increasing softness.[13,14]

It is worth comparing our experimental results with recent theory and simulation studies[17] of bulk 3D systems of Hertzian spheres, focusing at low temperature and increasing density. These studies predict a re-entrant fluid state (fluid–glass–fluid transition) with increasing density. While the prediction of a fluid to glass transition for Hertzian spheres is in agreement with our experimental observations, we do not observe a re-entrant fluid phase at higher ϕ_{eff} within our experimental range of densities.

This discrepancy points to the failure of a simple Hertzian model to describe the behaviour of microgel particles at very high densities $\phi_{\mathrm{eff}} \gg \phi_{\mathrm{cp}}$. Indeed, the simulations fail to reproduce the experimental $g(r)$ in this regime. As the internal core–shell structure might limit particle overlap, this could cause the potential to deviate from a simple Hertzian at close distances. However, it is important to point out that a re-entrant melting has also been predicted for other soft potentials.[18] Hence we believe that a systematic study of the particle size and structure as a function of ϕ_{eff} will be needed to establish the interaction potential and its possible dependence on ϕ_{eff}.

In summary, we have investigated the density-dependent bulk phase behavior of neutral PNIPAM microgel dispersions at a fixed temperature ($T = 15$ °C) for a wide range of ϕ_{eff} between $0.1 \leq \phi_{\mathrm{eff}} \leq 1.5$. The CLSM data clearly indicate that the fluid structure for $\phi_{\mathrm{eff}} \leq 0.52$ is in good agreement with a soft repulsive Hertzian interaction potential. At higher values of ϕ_{eff}, we found evidence for both fluid–crystal as well as fluid–glass transitions. When analyzing the density dependent pair-correlation function $g(r)$ in the fluid and glass phases, we found two characteristic structural signatures for the occurrence of the glass transition related to the height of the first peak $g_{\max}$ and the ratio $R = g_{\min}/g_{\max}$. Both exhibit non-monotonic behavior in the vicinity of the glass transition, and are obviously linked to the softness of the potential. The occurrence of a fluid–glass transition and observation of associated features in $g(r)$ are also in agreement with recent theoretical and simulation work on Hertzian spheres. However, we did not observe a reentrant fluid phase at high densities. It is clear that further systematic experimental and theoretical studies are required where these features are investigated as a function of the softness of the potential. Given the responsive nature of the microgels, it is also clear that we will need additional information on the relationship between the effective volume fraction and the swelling state of the particles when attempting to link our findings to existing theoretical and simulation work for high densities far above close packing.

This work was supported by the Swiss National Science Foundation and the Swedish Research Council (Project 621-2011-4338). EZ acknowledges support from ITN-234810-COMPLOIDS and MIUR-FIRB (Project RBFR125H0M).

References

1 P. N. Pusey and W. Van Megen, *Nature*, 2009, **320**, 340.
2 E. Zaccarelli, C. Valeriani, E. Sanz, W. C. K. Poon, M. E. Cates and P. N. Pusey, *Phys. Rev. Lett.*, 2009, **103**, 135704.
3 A. van Blaaderen and P. Wiltzius, *Science*, 1995, **270**, 117.
4 E. R. Weeks, J. C. Crocker, A. C. Levitt, A. Schotfield and D. A. Weitz, *Science*, 2000, **287**, 627.
5 W. K. Kegel and A. van Blaaderen, *Science*, 2000, **287**, 290.
6 U. Gasser, E. R. Weeks, A. Schotfield, P. N. Pusey and D. A. Weitz, *Science*, 2001, **292**, 258.
7 D. Heyes and A. Branka, *Soft Matter*, 2009, **5**, 2681.
8 C. N. Likos, H. Lowen, M. Watzlawek, B. Abbas, O. Jucknischke, J. Allgaier and D. Richter, *Phys. Rev. Lett.*, 1998, **80**, 4450.
9 E. Zaccarelli, C. Mayer, A. Asteriadi, C. N. Likos, F. Sciortino, J. Roovers, H. Iatrou, N. Hadjichristidis, P. Tartaglia, H. Löwen and D. Vlassopoulos, *Phys. Rev. Lett.*, 2005, **95**, 268301.
10 F. H. Stillinger, *J. Chem. Phys.*, 1976, **65**, 3968.
11 M. Watzlawek, H. Löwen and C. N. Likos, *J. Phys.: Condens. Matter*, 1998, **12**, 5087.
12 A. A. Louis, P. G. Bolhuis and J. P. Hansen, *Phys. Rev. E: Stat. Phys., Plasmas, Fluids, Relat. Interdiscip. Top.*, 2000, **62**, 7961.
13 D. M. Heyes, S. M. Clarke and A. C. Brańka, *J. Chem. Phys.*, 2009, **131**, 204506.
14 P. E. Ramirez-Gonzalez and M. Medina-Noyola, *J. Phys.: Condens. Matter*, 2009, **21**, 075101.
15 C. N. Likos, N. Hoffmann, H. Löwen and A. A. Louis, *J. Phys.: Condens. Matter*, 2002, **14**, 07681.
16 J. C. Pàmies, A. Cacciuto and D. Frenkel, *J. Chem. Phys.*, 2009, **131**, 044514.
17 L. Berthier, A. J. Moreno and G. Szamel, *Phys. Rev. B: Condens. Matter Mater. Phys.*, 2012, **82**, 060501(R).

18 A. Lang, C. N. Likos, M. Watzlawek and H. Löwen, *J. Phys.: Condens. Matter*, 2000, **12**, 5087.
19 P. Mohanty, D. Paloli, J. J. Crassous, and P. Schurtenberger, in *Hydrogel Micro- and Nanoparticles*, ed. L. Andrew Lyon and Michael J. Serpe, Wiley VCH, ISBN 978-3-527-33033-1, 2012, pp. 369–396.
20 M. Stieger, W. Richtering, J. S. Pedersen and P. Lindner, *J. Chem. Phys.*, 2004, **111**, 1705.
21 J. J. Lietor-Santos, B. Sierra-Martin, R. Vavrin, Z. Hu, U. Gasser and A. Fernández-Nieves, *Macromolecules*, 2009, **42**, 6225.
22 Z. Zhang, N. Xu, D. T. N. Chen, P. Yunker, A. M. Alsayed, K. B. Aptowicz, P. Habdas, A. J. Liu, S. R. Nagel and A. G. Yodh, *Nature*, 2009, **459**, 230.
23 F. Scheffold, P. Díaz-Leyva, M. Reufer, N. B. Braham, I. Lynch and J. L. Harden, *Phys. Rev. Lett.*, 2010, **104**, 128304.
24 D. D. Sessoms, I. Bischofberger, L. Cipelletti and V. Trappe, *Philos. Trans. R. Soc., A*, 2009, **367**, 5013.
25 J. R. Seth, L. Mohan, C. Locatelli-Champagne, M. Cloitre and R. T. Bonnecaze, *Nat. Mater.*, 2011, **10**, 838.
26 J. Mattsson, H. M. Wyss, A. Fernandez-Nieves, K. Miyazaki, Z. Hu, D. R. Reichman and D. A. Weitz, *Nature*, 2009, **462**, 83.
27 H. Senff and W. Richtering, *J. Chem. Phys.*, 1999, **111**, 1705.
28 J. Wu, B. Zhou and Z. Hu, *Phys. Rev. Lett.*, 2003, **90**, 048304.
29 P. S. Mohanty and W. Richtering, *J. Phys. Chem. B*, 2008, **112**, 14692.
30 P. Holmqvist, P. S. Mohanty, G. Nägele, P. Schurtenberger and M. Heinen, *Phys. Rev. Lett.*, 2012, **109**, 048302.
31 J. Riest, P. S. Mohanty, P. Schurtenberger and C. N. Likos, *Zeitschrift für Physikalische Chemie*, 2012, **226**, 711.
32 G. Romeo, L. Imperiali, J.-W. Kim, A. Fernández-Nieves and D. A. Weitz, *J. Chem. Phys.*, 2012, **136**, 124905.
33 U. Gasser, B. Sierra-Martin and A. Fernández-Nieves, *Phys. Rev. E Stat. Nonlin. Soft Matter Phys.*, 2009, **79**, 051403.
34 Z. Meng, J. K. Cho, V. Breedveld and L. A. Lyon, *J. Phys. Chem. B*, 2009, **113**, 4590.
35 M. Muluneh and D. A. Weitz, *Phys. Rev. E Stat. Nonlin. Soft Matter Phys.*, 2012, **85**, 021405.
36 J. J. Crassous, M. Siebenbürger, M. Ballauff, M. Drechsler, D. Hajnal, O. Henrich and M. Fuchs, *J. Chem. Phys.*, 2008, **128**, 204902.
37 A. Zaccone, J. J. Crassous, B. Béri and M. Ballauff, *Phys. Rev. Lett.*, 2011, **107**, 168303.
38 P. S. Mohanty, D. Paloli, J. J. Crassous, E. Zaccarelli and P. Schurtenberger, 2012, submitted.
39 J. Yang and K. S. Schweizer, *J. Chem. Phys.*, 2011, **134**, 204908.
40 H. H. Wendt and F. F. Abraham, *Phys. Rev. Lett.*, 1978, **41**, 1277.
41 J. L. Finney, *Proc. R. Soc. London, Ser. A*, 1970, **319**, 479.
42 B. V. R. Tata, P. S. Mohanty and M. C. Valsakumar, *Phys. Rev. Lett.*, 2002, **88**, 018302.
43 J. Brijitta, B. V. R. Tata, R. G. Joshi and T. Kaliyappan, *J. Chem. Phys.*, 2009, **131**, 074904.
44 T. Hellweg, C. D. Dewhurst, E. Brückner, K. Kratz and W. Eimer, *Colloid Polym. Sci.*, 2000, **278**, 972.